



Alpha–gamma discrimination by pulse shape in LaBr₃:Ce and LaCl₃:Ce

F.C.L. Crespi^{a,b}, F. Camera^{a,b,*}, N. Blasi^b, A. Bracco^{a,b}, S. Brambilla^b, B. Million^b, R. Nicolini^{a,b}, L. Pellegrini^a, S. Riboldi^{a,b}, M. Sassi^{a,b}, O. Wieland^b, F. Quarati^c, A. Owens^c

^a Università di Milano, Dipartimento di Fisica, Via Celoria 16, 20133 Milano, Italy

^b INFN sez. of Milano Via Celoria 16, 20133 Milano, Italy

^c Advanced Studies and Technology Preparation Division (SCI-PA), ESA/ESTEC Keplerlaan 1, 2201AZ Noordwijk, the Netherlands

ARTICLE INFO

Article history:

Received 18 December 2008

Received in revised form

13 January 2009

Accepted 18 January 2009

Available online 3 February 2009

Keywords:

LaBr₃ scintillators

LaCl₃ scintillators

Lanthanum halide

Gamma spectroscopy

Brilliance

Gamma detectors

Self-activity

PID

Alpha–gamma discrimination

Pulse Shape Analysis

ABSTRACT

The line-shape of the signals from LaBr₃:Ce and LaCl₃:Ce detectors coupled to PM tubes were studied. The possibility of discriminating the type of interacting radiation was investigated making use of Pulse Shape Analysis (PSA) techniques. The study was performed measuring the self-activity present in lanthanum halide crystals in coincidence with γ -rays in a HPGe crystal. A small but significant difference between α - and γ -induced signals was directly observed for both the crystals. Using a simple PSA algorithm, it was possible to emphasize the differences in the pulse shape of γ -rays and α -particles. This resulted in a rather clear identification of these two types of radiations.

© 2009 Elsevier B.V. All rights reserved.

1. Introduction

In the last few years, the lanthanum halide scintillators are attracting the scientific community in nuclear spectroscopy because of their ‘almost ideal’ scintillation properties. Recent studies have shown that LaBr₃:Ce material gives optimal energy resolution for scintillators (<3% at 662 keV), an excellent time resolution (\approx 300 ps), good efficiency [1–7] and a negligible variation of light output within the temperature range -20 to $+60$ °C [8]. The LaBr₃:Ce and LaCl₃:Ce crystals are commercially available from Saint Gobain Crystals under the brand name BrillanCe™, in particular, LaCl₃:Ce is named BrillanCe350 and LaBr₃:Ce is named BrillanCe380.

The availability of both LaBr₃:Ce and LaCl₃:Ce crystals (from now both addressed as BrillanCe™) in volumes larger than 1000 cc could make lanthanum halide scintillators a possible alternative to HPGe detectors for γ -ray measurements. In fact, if compared with HPGe, these crystals provide an excellent trade-off between efficiency and energy resolution, with, in addition, sub-nanosecond timing [9]. Such properties can be extremely useful in

situations in which the measured spectra are not very complex or in which the Doppler broadening, due to the velocity of the emitting source, is comparable to the resolution of BrillanCe™ detectors [10]. The sub-nanosecond time resolution, on the other hand, allows the measurement of Time of Flight with high resolution. This information is usually used for neutron– γ discrimination and for background rejection. The aforementioned situation can, for example, be found in specific in-beam measurements with fast exotic beams [10].

An aspect that is not yet fully investigated is the response, in terms of scintillation light, of BrillanCe™ crystals to light-charged particles. In fact, while there are several studies on the properties of these detectors, there is only one single research [11] on the pulse-shape discrimination capabilities of these scintillators. The work concentrated on the analysis of the pulse shapes for α -particles from ²⁴⁹Cf and for γ -rays from ²³²U source. The work shows the feasibility of γ – α discrimination in LaCl₃:Ce using the charge comparison methods but does not show any spectra corresponding to events selected using γ and α interaction.

The possibility to discriminate particles from γ -rays is an important issue in γ -spectroscopy or, more generally, in nuclear physics experiments.

In this work we compare the line-shape of signals generated by α -particles and γ -rays detected in both LaBr₃:Ce and LaCl₃:Ce scintillators. In addition, an algorithm to distinguish α -particles

* Corresponding author at: Università di Milano, Dipartimento di Fisica, Via Celoria 16, 20133 Milano, Italy.

E-mail address: camera@mi.infn.it (F. Camera).

from γ -rays is applied to the data and the corresponding results are discussed.

2. The identification technique

For the present study of γ -rays and α -particles identification, use is made of the internal radioactivity which is providing, simultaneously, both radiation types. In fact, the natural radioactivity induced by the ^{227}Ac decay chain is always present inside BrillanCe™ crystals. The employed technique is based on a coincidence measurement using a HPGe detector [12,13] together with a BrillanCe™ crystal. The α -particles-induced signal has been identified searching for events with energy between 1.5 and 3.0 MeV in BrillanCe™ crystals and, correspondingly, a γ -ray (measured in HPGe detector), which is a discrete transition of a nucleus in the decay chain of ^{227}Ac . The set of signals produced by γ -rays was selected searching for events that correspond to a single γ -ray of natural background, which is scattered in one detector and fully absorbed in the second (the sum of the two energy releases is the energy of the transition).

The adopted technique allows a perfect and unambiguous identification of the signals induced by low-energy α -particles and γ -rays. In addition, the selected events, even though generated by different types of radiations, were those that have produced exactly the same amount of scintillation light (measured as total energy in the spectroscopic amplifier, see the following section). As ^{227}Ac is supposed to be uniformly distributed inside the BrillanCe™ crystal, the method samples the scintillation properties of the whole crystal. It should be noted that by using a low-energy α -source, one would have sampled only the surface of the crystal, namely the region where the α -particles are fully stopped.

3. The measurement

Two crystals were used for this study: a $\text{LaCl}_3:\text{Ce}$ crystal, cylindrically shaped, with a diameter of 4" and 6" length and a 1" \times 1", cylindrically shaped $\text{LaBr}_3:\text{Ce}$ detector.

The $\text{LaCl}_3:\text{Ce}$ internal activity (measured in the range 0.07–3 MeV) is 1.9 cts/s/cc (0.04 cts/s/cc in the alpha region) while that of $\text{LaBr}_3:\text{Ce}$ is 4.4 cts/s/cc (0.5 cts/s/cc in the alpha region). The PM tubes coupled to the crystals were Photonis XP3540B02 ($\text{LaCl}_3:\text{Ce}$) and XP2060 ($\text{LaBr}_3:\text{Ce}$) with standard voltage dividers. In both cases, the crystals were encapsulated and the PMT was attached to the glass window of the capsule. The energy resolution at the 662 keV line of ^{137}Cs was 4.2% for $\text{LaCl}_3:\text{Ce}$ and 3.2% for $\text{LaBr}_3:\text{Ce}$.

In the measurements, the BrillanCe™ detectors were placed facing a HPGe detector (Tennelec CPVDS30-10195). Events which trigger both the HPGe and the BrillanCe™ allowed the DAQ system to acquire the total deposited energy in both detectors and to sample their pulse line-shapes. The total deposited energy was extracted using a Tennelec Tc244 (for HPGe detector) and a Camberra 2020 (for BrillanCe™) spectroscopic amplifiers and a CAEN V879 ADC. The detector pulses were acquired using a 12 bit CAEN V1729 ADC VME board with a sampling frequency of 2 GHz in a KMAX environment [14].

A matrix of the events with signals in both HPGe (on the x-axis) and $\text{LaBr}_3:\text{Ce}$ (on the y-axis) is displayed in Fig. 1. The horizontal (vertical) lines in Fig. 1 correspond to γ -rays that have deposited all their energy in HPGe ($\text{LaBr}_3:\text{Ce}$) in coincidence with radiation in $\text{LaBr}_3:\text{Ce}$ (HPGe). The diagonal lines at 45° , namely $E_{\text{HPGe}} + E_{\text{BrillanCe}} = \text{constant}$, are associated to single photons which enter in one detector and then scatter out and

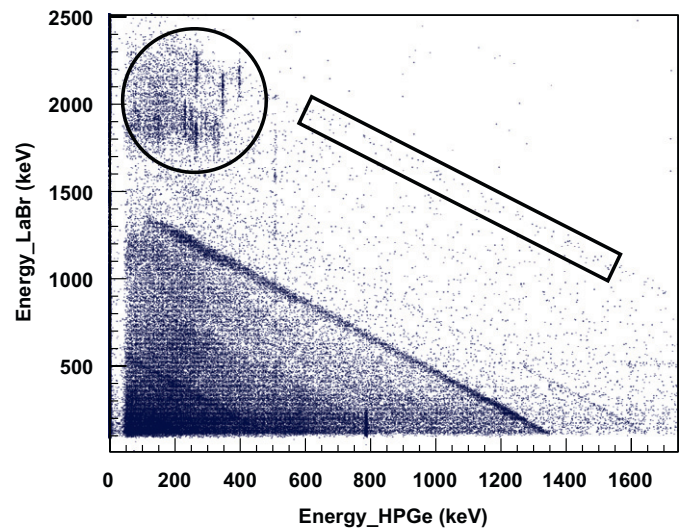


Fig. 1. The matrix of coincidence events measured with the $\text{LaBr}_3:\text{Ce}$ (y-axis) and with the HPGe (x-axis) detectors.

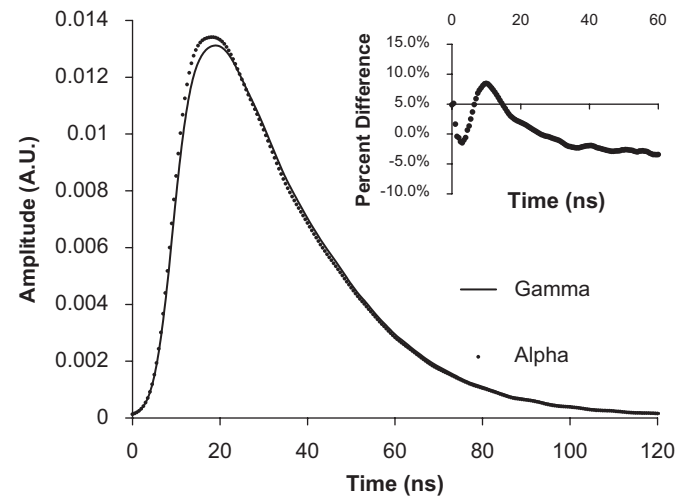


Fig. 2. The signal line-shapes measured for α -particles and γ -rays in a $\text{LaBr}_3:\text{Ce}$ detector. Each pulse is the result of an average of ≈ 300 pulses with the same energy measured using the spectroscopic amplifier. In the inset the ratio between the difference of the two signals and the alpha one, calculated in the interval 0–60 ns, is displayed.

are fully absorbed in the second detector. A similar matrix was obtained using the $\text{LaCl}_3:\text{Ce}$ crystal instead of $\text{LaBr}_3:\text{Ce}$.

Within the circular region in Fig. 1, some vertical lines are clearly visible. They are associated to events corresponding to alpha decays (measured in BrillanCe™ detectors) followed by discrete γ transitions (detected in HPGe).

As discussed in the previous section, the pulses associated to these events identify unambiguous signals produced in BrillanCe™ by α -particles. The events in the rectangular region of Fig. 1 identify the 2615 keV γ -rays from ^{208}Tl , which have scattered in one detector and are fully absorbed in the other. They were used as signals for γ -ray events. In Figs. 2 and 3 we present the comparison between the shape of the pulses measured for α -particles and γ -rays with $\text{LaBr}_3:\text{Ce}$ and $\text{LaCl}_3:\text{Ce}$ detectors. In the inset the relative ratio calculated around the maximum of the signal is shown. The pulses shown in the figures are averages of several hundreds of pulses measured directly at the anode of the PMT all having the same energy as obtained with the

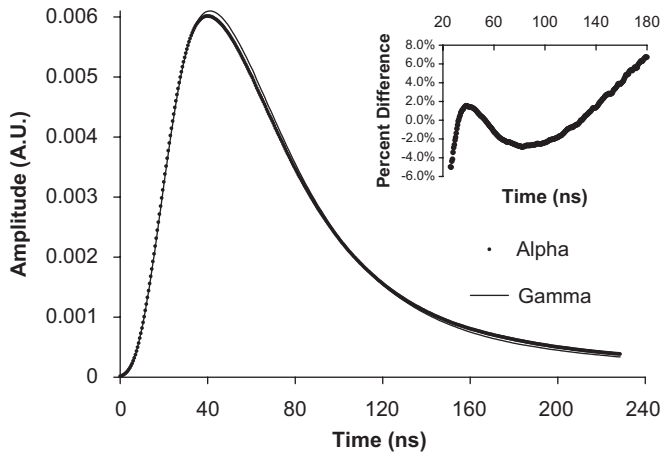


Fig. 3. The signal line-shapes measured for α -particles and γ -rays in a $\text{LaCl}_3:\text{Ce}$ detector. Each pulse is the result of an average of ≈ 1500 pulses with the same energy measured using the spectroscopic amplifier. In the inset the ratio between the difference of the two signals and the alpha one, calculated in the interval 20–180 ns, is displayed.

spectroscopic amplifier. No corrections for the bandwidth of the PMT or any kind of normalization of the pulses were applied.

The difference between an alpha- and a gamma-induced event is of the order of 10% maximum. An interesting feature is the fact that while in $\text{LaBr}_3:\text{Ce}$ the signal generated by α -particles is slightly faster than the one generated by γ -rays, in $\text{LaCl}_3:\text{Ce}$ exactly the opposite happens.

4. α - γ discrimination

As already discussed in Ref. [11], the expected difference in line-shape between alpha- and gamma-induced events is very small. In fact, BrillanCe™ crystals do not have different components within the scintillation light, like, for example, BaF_2 , which responds in a very different way if γ -rays or charged particles interact. However, by applying a simple algorithm, which uses a figure of merit I_0 we can clearly show that α -particles and γ -rays can be selected with reasonable efficiency (see Fig. 4).

The applied algorithm is based on the fact that the difference between the pairs of signals reported in Figs. 2 and 3 is concentrated in an interval around the maximum. In the adopted procedure the figure of merit I_0 is defined as

$$I_0 = \frac{\sum_{i=t_{\min}}^{t_{\max}} \text{trace}[i]}{A} \quad (4.1)$$

where t_{\min} and t_{\max} are, respectively, lower and upper boundaries of the interval in which the difference between the signals associated to alpha and gamma radiations is maximized (i.e. 10–30 ns for the case of $\text{LaBr}_3:\text{Ce}$ and 30–60 ns for $\text{LaCl}_3:\text{Ce}$). The value of A in relation (4.1) is the integral of the input trace (i.e. $\text{trace}[N]$, the signal sampled directly at the output of the PMT as described in Section 3) which is computed as

$$A = \sum_{i=t_0}^{t_0+N} \text{trace}[i] \quad (4.2)$$

In this relation N indicates the number of samples per signal and t_0 is the signal starting time. The value of t_0 was obtained using the leading-edge method on normalized pulses. It is important to stress that a good time alignment of signals is an important issue in order to properly compare their shapes.

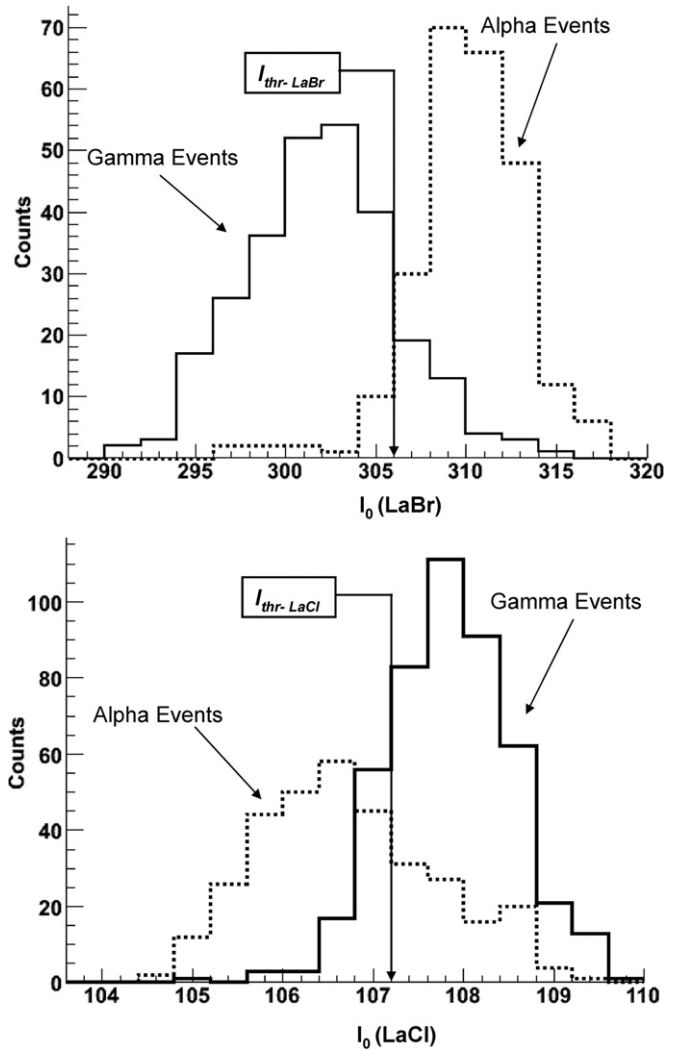


Fig. 4. The I_0 spectrum (see text) obtained applying the algorithm discussed in the text. In the bottom panel, which refers to $\text{LaCl}_3:\text{Ce}$, the peak on the left corresponds to alpha events while the one on the right corresponds to γ -ray events. Exactly the opposite happens in the top panel which refers to $\text{LaBr}_3:\text{Ce}$. The arrows show I_{thr} , namely the used threshold in I_0 to select α -particles or γ -rays.

Alternatively, the value of A can be obtained directly using the energy value measured in the electronic chain with the spectroscopic amplifier.

We have computed the I_0 value distributions for two datasets of purely alpha events and purely gamma events. These datasets were selected imposing appropriate conditions in the matrix of coincidence events measured with the $\text{LaBr}_3:\text{Ce}$ (or $\text{LaCl}_3:\text{Ce}$) and HPGe detectors (Fig. 1), using the identification technique described in Section 2. The resulting distributions are displayed in Fig. 4 (the two panels of the figure refer to the case of $\text{LaBr}_3:\text{Ce}$ and $\text{LaCl}_3:\text{Ce}$, respectively); in both cases two well-separated peaks appear: one is associated to α -particles events the other to γ -rays.

The fact that in each case the distributions are well separated shows that α -particles and γ -rays can be selected using the proposed algorithm, with reasonable efficiency.

As shown in the two panels of Fig. 4 (for both $\text{LaBr}_3:\text{Ce}$ and $\text{LaCl}_3:\text{Ce}$), I_{thr} corresponds to the value of I_0 for which the uncertainty in the alpha/gamma discrimination is maximum. The I_{thr} value extracted in this way can then be used for discriminating alphas and gammas in any other independent measure (namely for a $\text{LaBr}_3:\text{Ce}$ detector if $I_0 > I_{\text{thr}}$ then the processed signal is

associated to an alpha particle, otherwise to a gamma; just the opposite is done in the case of using a LaCl₃:Ce detector).

An event-by-event comparison between the measured I_0 and the threshold value I_{thr} placed between the two distributions allows a α - γ discrimination with a high level of accuracy. It is clear that the degree of accuracy of the α - γ discrimination depends on the value of I_{thr} and on the relative ratio between the

intensities of the α and γ emissions. In the present case it was possible to identify $\approx 90\%$ (in LaBr₃:Ce) and $\approx 75\%$ (in LaCl₃:Ce) of the measured particles.

The matrixes displayed in Fig. 5 show the region of Fig. 1 selected with the circle without any condition (top panel) on I_0 , selecting γ -rays (central panel) or α -particles (bottom panel). The plots clearly show that a good, although not perfect, identification

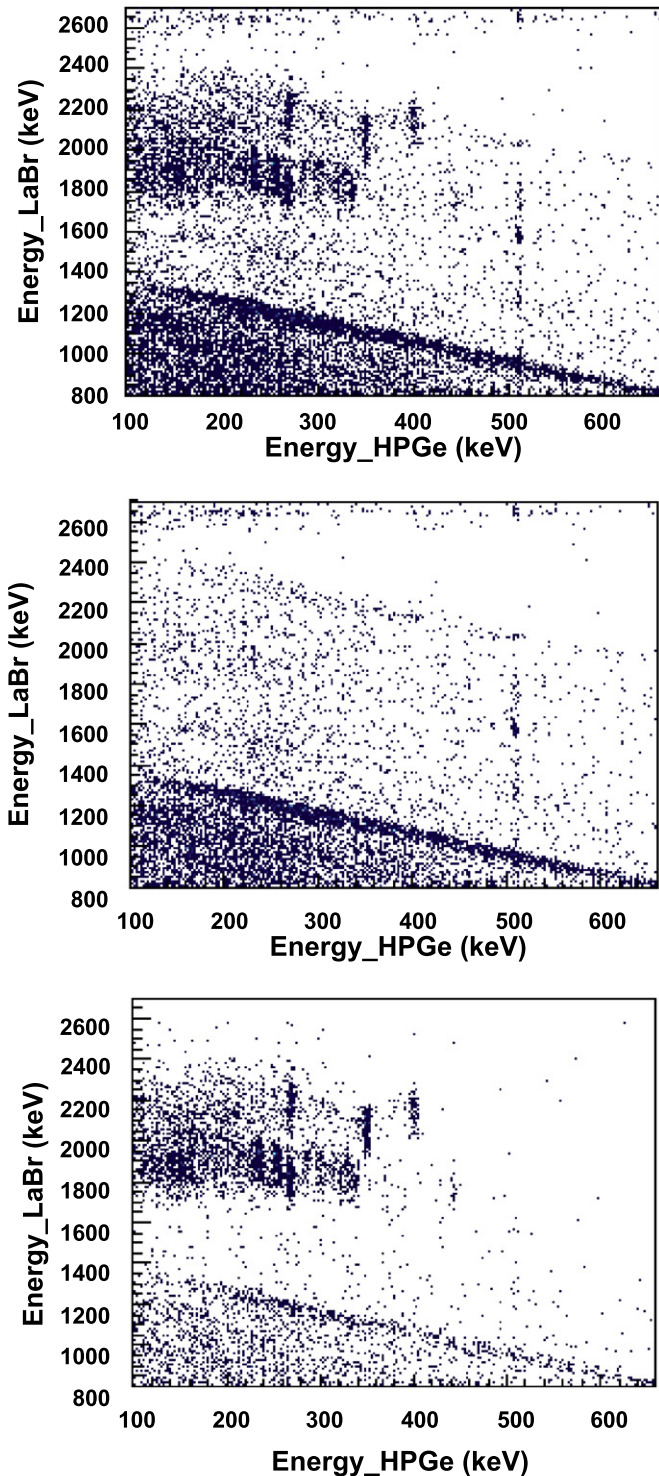


Fig. 5. A blow-up of the region selected by the circle in Fig. 1 when no condition on I_0 is applied (top panel), selecting γ -rays ($I_0 < I_{thr}$ —central panel) and selecting α -particles ($I_0 > I_{thr}$ —bottom panel).

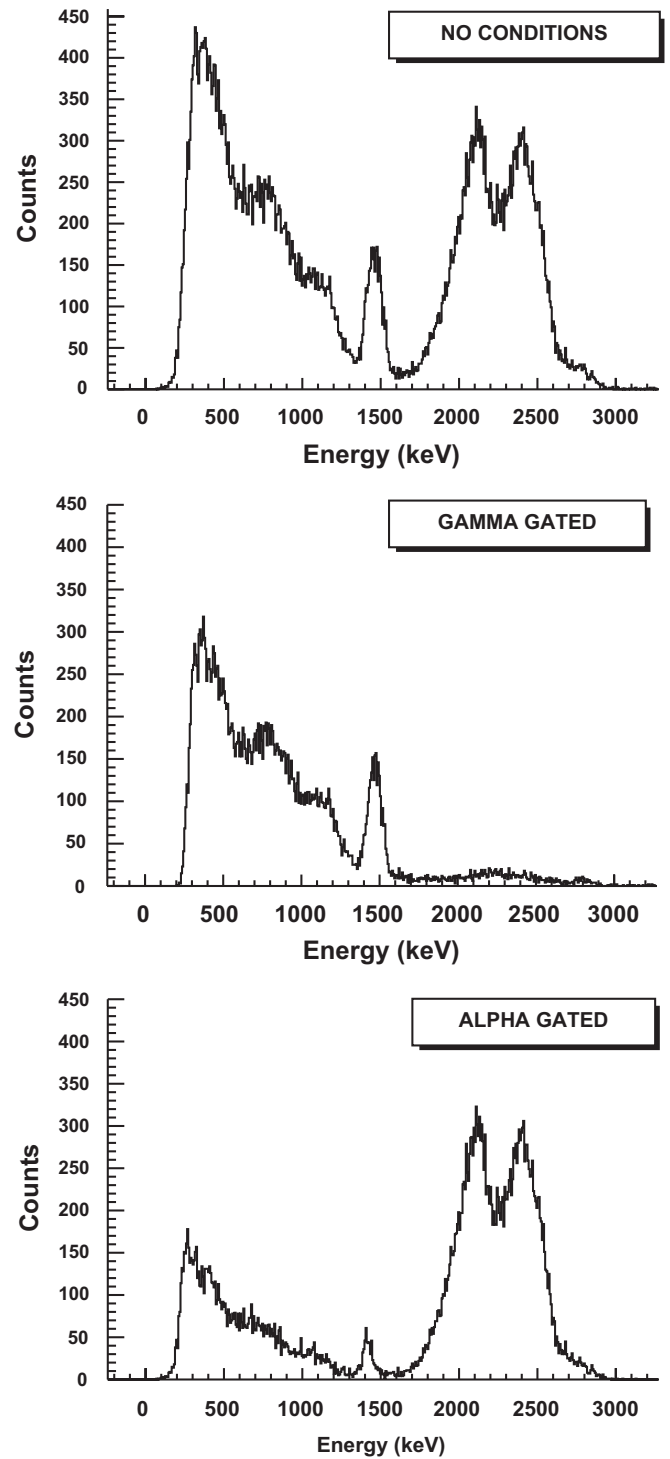


Fig. 6. The internal radioactivity and natural background spectra measured with the LaBr₃:Ce detector. The top panel spectrum shows the measurement in single with no condition on I_0 (see text). Middle and bottom panels show the spectra obtained by placing alpha or gamma ray conditions on I_0 through Pulse Shape Analysis.

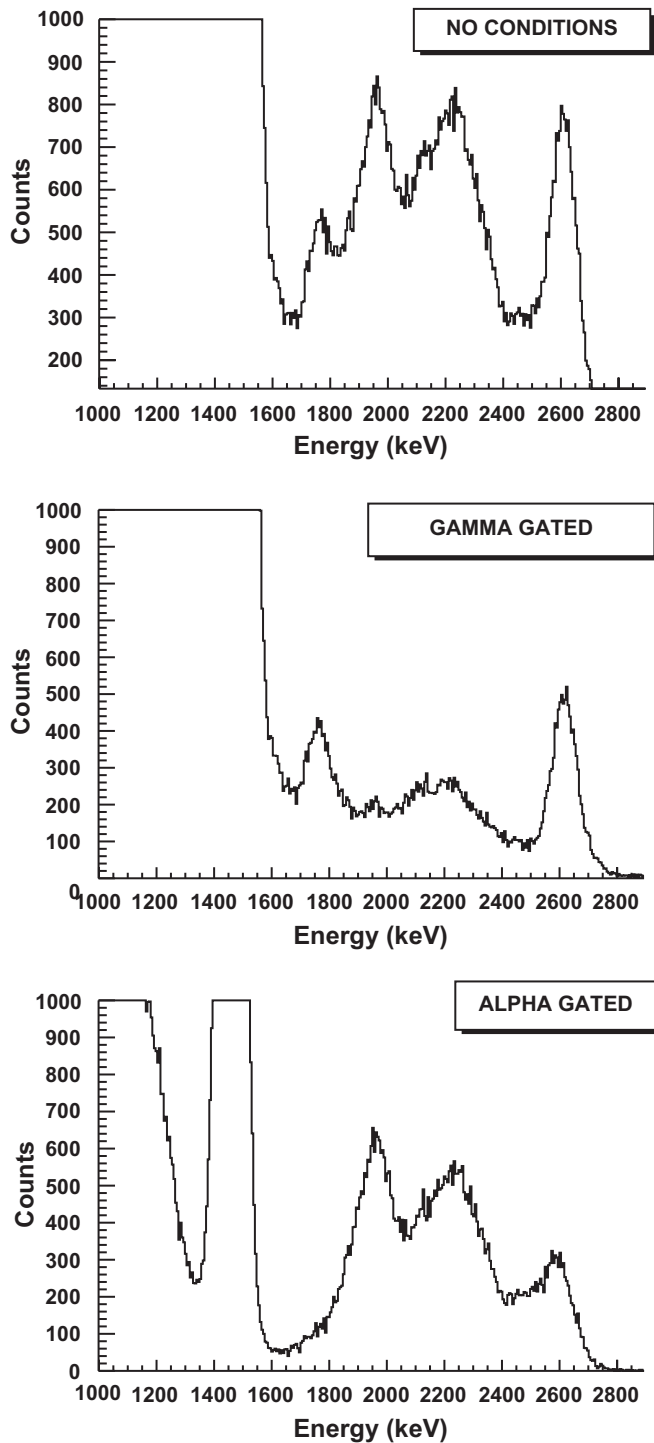


Fig. 7. The internal radioactivity and natural background spectra measured with the $\text{LaCl}_3:\text{Ce}$ detector. The top panel spectrum shows the measurement in single with no condition on I_0 (see text). Middle and bottom panels show the spectra obtained by placing alpha or gamma ray conditions on I_0 through Pulse Shape Analysis.

of the nature of the interacting particle was achieved. Very similar results were obtained for the $\text{LaCl}_3:\text{Ce}$ detector although, as expected from Fig. 4, the α - γ discrimination is somewhat less selective.

As a final check we have applied the algorithm to the pulses of $\text{LaBr}_3:\text{Ce}$ and $\text{LaCl}_3:\text{Ce}$ detectors measured in singles, namely without any coincidence condition.

In Figs. 6 and 7 the energy spectra extracted from this dataset are displayed.

The top panels show the internal radioactivity plus natural background spectra measured in singles with the BrillanCe™ detectors. Both spectra show, between 1.5 and 2.8 MeV, the contribution due to the alpha decays from the ^{227}Ac chain. In the case of $\text{LaBr}_3:\text{Ce}$ detector the alpha activity is 10 times stronger than that of the $\text{LaCl}_3:\text{Ce}$ and the energy spectrum of the alpha part, if compared with that of Refs. [12,13], does not show the strong peak centred at 2.8 MeV. The peak is produced by the alpha decay of ^{215}Po (half-life 1.9 ms, $E_\alpha = 7386$ keV). Such decay has a lifetime shorter than the length of the busy signal of the acquisition (30 ms). Consequently, every time ^{215}Po decayed, the acquisition was already busy processing the data from the mother isotope ^{219}Rn and, consequently, the event could not be acquired and processed. In the case of $\text{LaCl}_3:\text{Ce}$ detector, instead, the 2.8 MeV peak from the ^{215}Po alpha particle is substituted by the 2615 keV gamma line from the decay of ^{208}Tl , which is present in the natural background. This peak is very weak in $\text{LaBr}_3:\text{Ce}$ spectrum because of the small volume of the detector.

The middle panel of Figs. 6 and 7 shows the spectra produced requiring the ‘ γ -ray’ condition. In the $\text{LaCl}_3:\text{Ce}$ spectrum the 1765 and 2615 keV peaks are clearly visible together with the 2615 keV Compton shoulder while in $\text{LaBr}_3:\text{Ce}$ spectrum almost no counts remain. Finally, the bottom panels of the figures show the ‘alpha’-gated spectra. From the comparison between middle and bottom panels it is clear that the used algorithm was capable of achieving a rather good alpha–gamma selection.

5. Conclusion

In this study we have compared the signal shape produced by α -particles and γ -rays in BrillanCe™ $\text{LaBr}_3:\text{Ce}$ and $\text{LaCl}_3:\text{Ce}$ detectors. The comparisons have shown that, with the used crystals, a small difference is present and that, as the displayed plots clearly show, this is sufficient to allow a good identification of the nature of the interacting particles. A further and extremely interesting step in the same direction is the measurement of the pulse shapes induced by neutrons, protons and heavy ions. These studies widen the application fields of BrillanCe™ detectors in both nuclear physics and its applications.

References

- [1] C.M. Rosza, et al., Performance summary: BrillanCe™ scintillators LaCl_3 and LaBr_3 , Saint Gobain crystals, available at [/www.detectors.saint-gobain.com](http://www.detectors.saint-gobain.com).
- [2] E.V.D. van Loef, et al., Nucl. Instr. and Meth. A 486 (2002) 254.
- [3] P. Menge, et al., Nucl. Instr. and Meth. A 579 (2007) 6.
- [4] J. Glodo, et al., IEEE Trans. Nucl. Sci. NS-52 (2005) 1805.
- [5] F. Quarati, et al., Nucl. Instr. and Meth. A 574 (2007) 115.
- [6] W.W. Moses, Nucl. Instr. and Meth. A 487 (2002) 123.
- [7] K.S. Shah, et al., IEEE Trans. Nucl. Sci. NS-51 (2004) 2395.
- [8] M. Moszynski, et al., Nucl. Instr. and Meth. A 568 (2006) 739.
- [9] M. Moszynski, et al., Nucl. Instr. and Meth. A 567 (2006) 31.
- [10] D. Weisshaar, et al., Nucl. Instr. and Meth. A 594 (2008) 56.
- [11] C. Hoel, et al., Nucl. Instr. and Meth. A 540 (2005) 205.
- [12] R. Nicolini, et al., Nucl. Instr. and Meth. A 582 (2007) 554.
- [13] B.D. Milbrath, et al., Nucl. Instr. and Meth. A 547 (2005) 504.
- [14] S. Brambilla, et al., Sparrow Corporation Data Acquisition Conference and Workshop, 22–24 March 2005, Daytona Beach, FL, 2005.